Tree Physiology 36, 643–652
doi:10.1093/treephys/tpv116

Technical note

Distribution of coniferin in differentiating normal and compression woods using MALDI mass spectrometric imaging coupled with osmium tetroxide vapor treatment

Arata Yoshinaga[1,3], Hiroshi Kamitakahara[2] and Keiji Takabe[1]

[1]Laboratory of Tree Cell Biology, Division of Forest and Biomaterials Science, Graduate School of Agriculture, Kyoto University, Sakyo-ku, Kyoto 606-8502, Japan;
[2]Laboratory of The Chemistry of Biomaterials, Division of Forest and Biomaterials Science, Graduate School of Agriculture, Kyoto University, Sakyo-ku, Kyoto 606-8502, Japan;
[3]Corresponding author (aryosshy@kais.kyoto-u.ac.jp)

Received April 18, 2015; accepted October 2, 2015; published online October 27, 2015; handling Editor Hans-Peter Mock

Matrix-assisted laser desorption/ionization mass spectrometric imaging (MALDI-MSI) was employed to detect monolignol glucosides in differentiating normal and compression woods of two Japanese softwoods, *Chamaecyparis obtusa* and *Cryptomeria japonica*. Comparison of matrix-assisted laser desorption/ionization time-of-flight mass spectrometry collision-induced dissociation fragmentation analysis and structural time-of-flight (MALDI-TOF CID-FAST) spectra between coniferin and differentiating xylem also confirmed the presence of coniferin in differentiating xylem. However, as matrix-assisted laser desorption/ionization time-of-flight mass spectrometry (MALDI-TOF MS) and MALDI-TOF CID-FAST spectra of sucrose were similar to those of coniferin, it was difficult to distinguish the distribution of coniferin and sucrose using MALDI-MSI and collision-induced dissociation measurement only. To solve this problem, osmium tetroxide vapor was applied to sections of differentiating xylem. This vapor treatment caused peak shifts corresponding to the introduction of two hydroxyl groups to the C=C double bond in coniferin. The treatment did not cause a peak shift for sucrose, and therefore was effective in distinguishing coniferin and sucrose. Thus, it was found that MALDI-MSI combined with osmium tetroxide vapor treatment is a useful method to detect coniferin in differentiating xylem.

Keywords: *Chamaecyparis obtusa*, compression wood, coniferin, *Cryptomeria japonica*, lignification, MALDI-TOF-MS.

Introduction

Lignin is a dehydrogenative polymer of monolignols, including *p*-coumaryl, coniferyl and sinapyl alcohols. Lignification allows the plant cell wall to be more hydrophobic, more pressure resistant and more decay resistant against microorganisms. These monolignols are thought to be synthesized within the cell, transported to cell walls and polymerized with the aid of enzymes such as peroxidase and laccase (Liu 2012). The lignification process has been examined in softwood tracheid cell walls by ultraviolet microscopy, fluorescence microscopy, microautoradiography and transmission electron microscopy (Wardrop 1957, Kutscha and Schwarzmann 1975, Imagawa et al. 1976, Takabe et al. 1981*a*, *b*, 1985, 1986). This process can be divided into the following three stages: (i) lignification of the cell corner middle lamella and primary walls during S_1 layer formation; (ii) slow lignification of the primary walls and the outer part of the secondary walls during S_2 and S_3 layer formation; and (iii) very active lignification throughout the secondary walls after S_3 layer formation. As most of the analytical techniques applied are based on chemical fixation and dehydration through an ethanol series during specimen preparation, the cellular distribution of monolignols extracted during preparation has not been elucidated.

Monolignol glucosides, such as coniferin, have been considered participants in lignification (Freudenberg and Harkin 1963,

Freudenberg and Torres-Serres 1967, Terazawa et al. 1984). Based on incorporation of radiolabeled monolignol glucosides (*p*-glucocoumaryl alcohol, coniferin and syringin) in differentiating xylem, the lignification process in softwood cell walls has been studied by microautoradiography (Terashima and Fukushima 1988, Fukushima and Terashima 1991). It could be concluded that these monolignol glucosides contribute to lignification in vivo. The cambial sap of *Picea excelsa* (Freudenberg and Harkin 1963) and that of six other gymnosperm species (Terazawa et al. 1984) contains coniferin. Coniferin distribution in serial tangential sections prepared from differentiating xylem of 2-year-old shoots of *Pinus thunbergii* was examined by Fukushima et al. (1997). The examination showed that most of the coniferin existed in the developing cells during the early stages of differentiation.

Coniferin is synthesized by coniferyl alcohol glucosyltransferase from coniferyl alcohol and uridine diphosphate glucose. This enzyme was detected in hypocotyls from 10-day-old spruce (*Picea abies* (L.) Karst.) seedlings (Schmid et al. 1982), in the cambial zone of *Pinus strobus* (Steeves et al. 2001), and in the cambial zone and differentiating xylem of *Pinus banksiana* (Savidge and Forster 1998).

Coniferin-β-glucosidase is an enzyme that hydrolyses coniferin to coniferyl alcohol and glucose. This enzyme was isolated from seedlings of *P. abies* (Marcinowski et al. 1979), from the seeds of *Glycine max* (Hösel and Todenhagen 1980) and from differentiating xylem of *Pinus contorta* var *latifolia* (Dharmawardhana et al. 1995). Dharmawardhana et al. (1995) showed that this enzyme specifically hydrolyses coniferin to produce coniferyl alcohol and demonstrated its activity in the cell walls of differentiating xylem. They suggested that coniferin may be transported to the cell wall, where it is hydrolysed by coniferin-β-glucosidase to coniferyl alcohol. Marjamaa et al. (2003) reported that β-glucosidase activity was highest in May and confirmed that this enzyme participates in lignification. Samuels et al. (2002) used immunoelectron microscopy to localize β-glucosidase in tracheid secondary cell walls of lodgepole pine.

Accordingly, the involvement of coniferin in lignification has been well demonstrated, but the transportation mechanism of monolignols (or monolignol glucosides) remains unclear (Liu 2012). Recently, Tsuyama et al. (2013) demonstrated the involvement of a common endomembrane-associated proton/coniferin antiport mechanism in the lignifying tissues of woody plants (both angiosperms and gymnosperms). Chapelle et al. (2012) reported that knockout mutants of *BGLU45* and *BGLU46*, genes encoding stem-specific β-glucosidases, in *Arabidopsis thaliana* did not have a lignin-deficient phenotype. They suggested that monolignol glucosides are the storage form of monolignols in *Arabidopsis*. Clarification of the cellular distribution of monolignols or monolignol glucosides is needed.

We examined the cellular distribution of coniferin using Raman microscopy and scanning electron microscopy and showed that in tracheid lumina during S_2 layer formation, a considerable amount of coniferin existed as needle-like crystals (Morikawa et al. 2010). Since Raman peaks of coniferin and those of lignified cell walls were quite similar except for a few peak with low intensity, it was difficult to get an image showing coniferin distribution within one section of differentiating xylem using Raman microscopy. Moreover, the main Raman spectra of the three kinds of glucosides are quite similar, making it difficult to distinguish among the glucosides when they are present together.

Matrix-assisted laser desorption/ionization mass spectrometic imaging (MALDI-MSI) is an effective technique for visualizing the distribution of various substances representing a very wide range of molecular masses, from low molecular mass metabolites to proteins. This technique has been widely applied in studying animal and plant cells. The application of MALDI-MSI in plant biology has been reviewed by Kaspar et al. (2011) and Peukert et al. (2012). Recently, this technique was applied to study the metabolite distribution in roots and root nodules of *Medicago truncatula* during nitrogen fixation (Ye et al. 2013). Li et al. (2010) obtained images of saccharide-related ions in *Miscanthus* × *giganteus* using MALDI-MSI. For trees, Lunsford et al. (2011) applied MALDI-MSI to analyse cellulose and hemicellulose in poplar tissue. Araújo et al. (2014) applied MALDI-MSI to the sections of *Eucalyptus globulus* and *Eucalyptus grandis* to visualize the distribution of three kinds of monolignols, namely *p*-coumaryl, coniferyl and sinapyl ancohol, in young stems. Although the lateral resolution of MALDI-MSI is lower than that of other techniques, such as time-of-flight secondary ion mass spectrometry (TOF-SIMS, for e.g., Jung et al. 2012) and Raman microscopy, this technique is suitable for clarifying the distribution of monolignol glucosides in differentiating xylem. Thus, in the present study, we used MALDI-MSI to clarify the distribution of coniferin during lignification in differentiating xylem of two Japanese softwoods, *Chamaecyparis obtusa* and *Cryptomeria japonica*, which are important tree species in Japan. Moreover, we examined compression wood that contains higher amount of lignin and also *p*-hydroxyphenyl lignin in addition to guaiacyl lignin. Therefore another aim of the present study was to determine if accumulation of a higher amount of coniferin or *p*-glucocoumaryl alcohol occurs in differentiating compression wood.

Materials and methods

Plant materials

A 22-year-old Japanese cypress (*C. obtusa*, height 11.95 m, diameter of breast height (DBH) 13.1 cm) and a 24-year-old Japanese cedar (*C. japonica*, height 9.29 m, DBH 13.2 cm) were harvested during active cell wall formation in mid-June and at the end of May, respectively. These trees grew upright and produced normal wood. A 19-year-old *C. japonica* (height 2.80 m, DBH 3.6 cm) was artificially inclined at 30–45° at the

end of March and harvested during the middle of June. An 8-year-old *C. obtusa* (height 2.87 m, DBH 1.8 cm), naturally inclined at ~70°, was also harvested during the middle of June. The last two trees produced compression wood. The upright Japanese cypress was the same tree we used in the paper by Morikawa et al. (2010) to examine coniferin distribution by Raman microscopy. The tree samples from that study were stored at −30 °C. After the trees were felled, several wood discs were collected at breast height of the trunk. Small blocks containing the inner bark, cambial zone and differentiating xylem were collected from the discs. These blocks were stored in a wet box to avoid drying until they were sectioned for MALDI-MSI analysis.

Preparation of samples for MALDI-MSI

Transverse sections (20 μm thick) were cut from the blocks with a sliding microtome (Yamato Koki Ltd, Asaka, Japan). Because the sections were frequently split in the zone where cells are enlarging with the very thin primary walls, it was difficult to cut sections containing both inner bark and differentiating xylem. To avoid contamination due to overlap of the split inner bark section, inner bark was manually removed before sectioning. Sections were placed on a glass slide so that contact between wet differentiating xylem and the surface of the glass slide was minimized to avoid moving free substances, including monolignol glucosides, onto the glass slide surface. Sections were then air dried and dried in vacuo. During air drying, monolignol glucosides within the lumen of developing tracheid were expected to be fixed in the area from the lumen to the developing cell wall. Dried sections were fixed with a sheet of carbon double-sided tape (Nisshin EM, Japan ~110 μm thick) on the stainless steel target plate (Bruker Daltonics, Yokohama, Japan, MTP384 ground steel, cat. no. 209519), which was specially processed to a depth of ~120 μm (Figure 1). The original surface of the target plate was placed in the middle depth of the sections, and peak shifts of the MS spectra due to the thickness of sections were minimized.

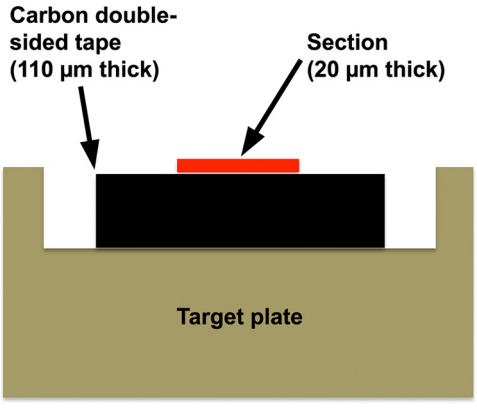

Figure 1. A schematic drawing of a specially processed target plate used for the present study. The plate was processed so the section was fixed on the original plane of the target plate.

Treatment by osmium tetroxide vapor

To distinguish the presence of coniferin and sucrose, osmium tetroxide vapor was applied in MALDI-MSI. Transverse sections (20 μm) of *Populus euramericana* mature sapwood were cut, washed in water and ethanol to remove soluble compounds, dried and used as a model section of similar condition to the section from differentiating xylem. A few drops of aqueous solution of *p*-glucocoumaryl alcohol, coniferin, syringin or sucrose (1 mg ml^{-1}) were placed on the sections and air dried. The parts of the sections for MALDI-MSI were placed in a glass vial containing a small amount of 4% osmium tetroxide aqueous solution, sealed and treated by vapor for 24–72 h at room temperature. Treated sections were removed from the vial, air-dried and then dried in vacuo. The sections were fixed on a target plate as described above for subsequent MALDI-MSI.

Spraying of matrix on the sections

To prepare a matrix solution for MALDI-MSI, three kinds of solutions were prepared: (i) 2,5-dihydroxybenzoic acid (DHB; Tokyo Kasei Co., Ltd, Japan; 100 mg ml^{-1}) in acetonitrile/water (1 : 1); (ii) sodium trifluoroacetic acid (NaTFA; 20 mg ml^{-1}) in acetonitrile/water (1 : 1); and (iii) leucine enkephalin (1 mg ml^{-1}) in acetonitrile/water (1 : 1). Solution 1 was a matrix for MALDI-TOF MS, and Solution 2 was added as a cationized reagent. Since coniferin gave two peaks corresponding to sodium adduct $[M + Na]^+$ and potassium adduct $[M + K]^+$, the addition of Solution 2 caused a peak shift to the peak of sodium adduct $[M + Na]^+$, enabling us to simplify peak interpretation. Solution 3 was added as an internal standard compound with a known relative molecular mass ($M_r = 555.62$) to confirm a peak shift due to slight curling of sections. These three solutions were mixed at a ratio of 1 : 2 : 3 = 5 : 5: 1 and sprayed on the surface of the sections with an airbrush (PS274, GSI Creos Corporation, Tokyo, Japan). For calibration, an aqueous solution of polyethylene glycol (PEG) 600 (BioUltra grade, Sigma; 1 mg ml^{-1}) and DHB (10 mg ml^{-1}) was mixed 1 : 1 and put on the same target plate. The target plate was dried in vacuo before MALDI-MSI analysis.

MALDI-MSI

Measurements of MALDI-MSI were carried out by MALDI-TOF MS (Bruker Daltonics Autoflex III). All spectra were measured in the reflection-positive ion mode using external calibration (PEG 600). Imaging measurements were performed with fleximaging software (Bruker Daltonics). Measurements were made in 50-μm increments and mass range of 0–1000 Da. To avoid the effect of large peaks due to a matrix, measurements were recorded in a matrix-suppression mode so that peaks from $m/z < 250$ were deflected to detect efficiently other peaks, including coniferin.

Measurement of MALDI-TOF CID-FAST spectra

To obtain further information on chemical structure as well as m/z, matrix-assisted laser desorption/ionization time-of-flight

mass spectrometry collision-induced dissociation fragmentation analysis and structural TOF (MALDI-TOF MS CID-FAST), spectra were measured from sections without treatment with osmium tetroxide. Collision-induced dissociation (CID) spectra were also recorded from authentic *p*-glucocoumaryl alcohol, coniferin, syringin and sucrose. Argon gas was introduced in the system at a pressure of 6.0 x 10^{-4} Pa (6.0×10^{-6} mbar), and the fragmentation pattern from the section was compared with authentic compounds.

Light and fluorescence microscopy

Parts of the 20-μm-thick transverse sections were stained with safranin and astra blue, mounted with canada balsam and observed under a light microscope to examine general anatomical structures of differentiating xylems. To study the lignification process, a part of the 20-μm-thick sections was stained with phloroglucinol hydrochloric acid (Wiesner reaction) and observed under a light microscope. To examine distribution of substances that show autofluorescence, such as coniferin or coniferyl alcohol and other lignin-related compounds, parts of the 50-μm-thick sections were mounted on glass slides, and coverslips were placed on the sections without mounting medium. The edge of the coverslip was fixed with a strip of tape to prevent curling of the sections, and sections were observed under a fluorescence microscope (Olympus BX-51) with the filter set of Omega XF06 (Omega Optical Inc., Brattleboro, VT, USA)

Results

MALDI-MSI of differentiating xylem in normal wood

Figure 2 shows MALDI-TOF MS spectra of the monolignol glucosides *p*-glucocoumaryl alcohol, coniferin, and syringin. These three glucosides showed two peaks corresponding to their sodium and potassium adducts (*p*-glucocoumaryl alcohol: *m/z* 335 $[M + Na]^+$ and 351 $[M + K]^+$; coniferin: *m/z* 365 $[M + Na]^+$ and 381 $[M + K]^+$; syringin: *m/z* 395 $[M + Na]^+$ and 411 $[M + K]^+$). From water extracts of differentiating xylem in *C. obtusa* normal wood, two distinct peaks at *m/z* 365 $[M + Na]^+$ and *m/z* 381 $[M + K]^+$ were detected (Morikawa et al. 2010). To simplify the interpretation of results from MALDI-MSI, NaTFA was added as a cationized reagent to shift the two peaks from coniferin in differentiating xylem to the single peak at *m/z* 365 $[M + Na]^+$.

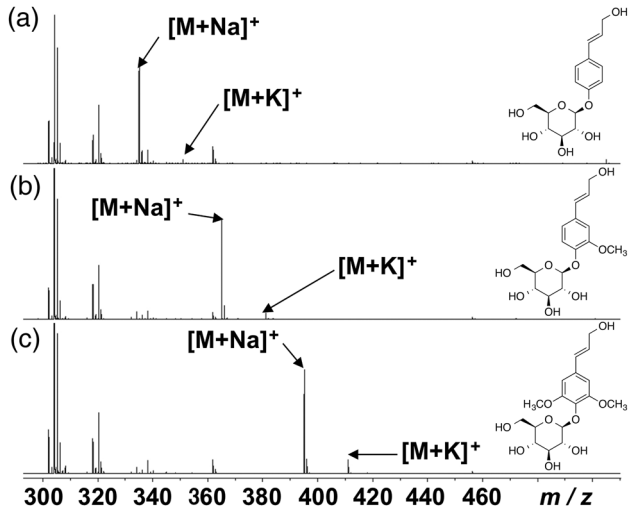

Figure 2. MALDI-TOF MS spectra of *p*-glucocoumaryl alcohol (a), coniferin (b) and syringin (c) taken with DHB as a matrix.

The results of MALDI-MSI in normal wood in *C. obtusa* are shown in Figure 3. The abundance of the *m/z* 365 product (similar to coniferin $[M + Na]^+$) was specific to the developing xylem during S_2 layer formation (Figure 3c). The peaks of *m/z* 335 (similar to *p*-glucocoumaryl alcohol $[M + Na]^+$) and *m/z* 395 (similar to syringin $[M + Na]^+$) were very weak, and their images were not clear (Figure 3b and d).

Comparison of the MALDI-MSI image with light and fluorescence micrographs is provided in Figure 4. The area showing abundance of the *m/z* 365 product (similar to coniferin $[M + Na]^+$) showed blue color under safranin astra blue staining (Figure 4b), weak red-purple color under Wiesner staining (Figure 4c) and slightly stronger autofluorescence (Figure 4d). These results agree well with those of Morikawa et al. (2010), who showed that coniferin was mainly distributed in tracheid lumina during S_2 layer formation.

Comparison of MALDI-TOF CID-FAST spectra

Figure 5a–c shows MALDI-TOF CID-FAST spectra from *p*-glucocoumaryl alcohol, syringin and coniferin, respectively. These three monolignol glucosides showed different fragmentation patterns. A MALDI-TOF CID-FAST spectrum from a distinct peak of *p*-glucocoumaryl alcohol at *m/z* 335 as a precursor ion showed major peaks at *m/z* 156.2, 171.1, 176.6 and 295.3 as product ions, and that from a distinct peak of syringin at *m/z* 395 as a precursor ion had major peaks at *m/z* 185.3, 192.7, 232.3, 233.5 and 364.3 as product ions. The peaks at *m/z* 185.3 and *m/z* 233.5 probably originated from a glucose moiety and a sinapyl alcohol moiety, respectively. The result of MALDI-MSI normal wood in *C. obtusa* described above suggests the presence of coniferin in differentiating xylem. However, there remains the possibility that other compounds showing similar *m/z* may also exist in differentiating xylem. Therefore, the CID spectrum was measured for differentiating xylem and compared with coniferin. Furthermore, the CID spectrum was compared with that of sucrose, which was also reported to exist in differentiating xylem (Terazawa et al. 1984).

Figure 5c shows a MALDI-TOF CID-FAST spectrum from a distinct peak of coniferin at *m/z* 365 as a precursor ion. Three major peaks at *m/z* 185.2, 201.2 and 202.2 and two minor peaks at *m/z* 163.0 and 344.6 were detected as product ions. The two major peaks at *m/z* 185.3 and 203.2 and one minor

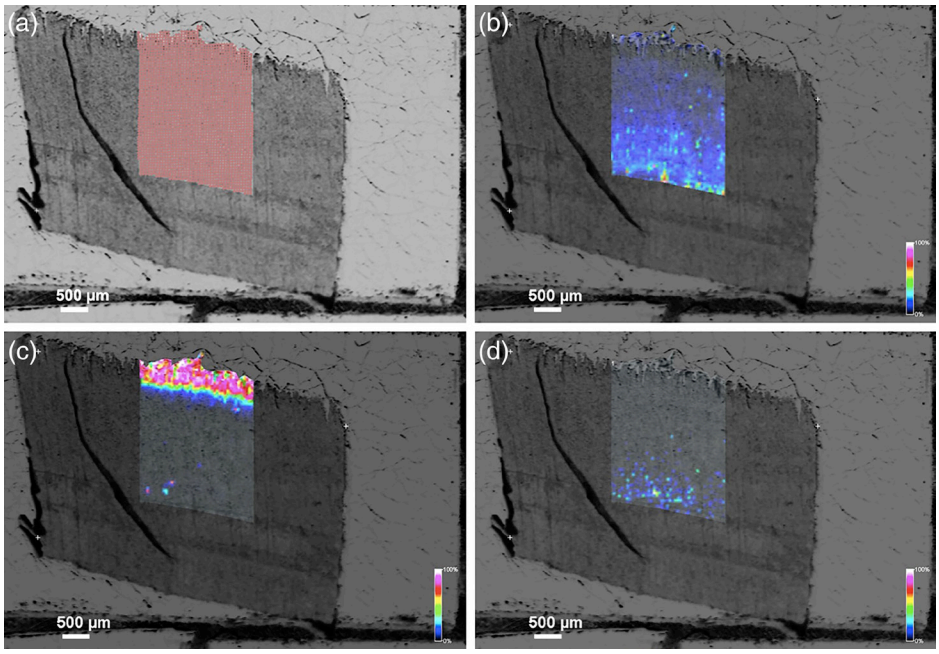

Figure 3. Ion images obtained from MALDI-MSI of a transverse section from differentiating normal wood of *C. obtusa*. (a) An image of a transverse section showing the area of measurement. (b–d) Ion images obtained from MALDI-MSI showing distribution of the *m/z* 335 (b), 365 (c) and 395 (d) products. The abundance of the *m/z* 365 product was mainly found in developing xylem during S_2 layer formation (c).

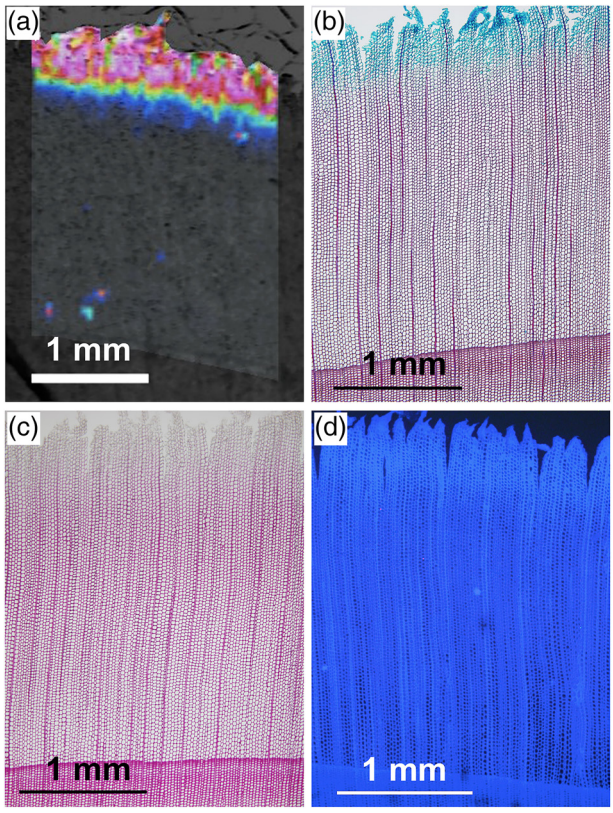

Figure 4. Comparison between an ion image obtained from MALDI-MSI and light and fluorescence micrographs. (a) An ion image obtained from MALDI-MSI showing distribution of the *m/z* 365 product (enlarged from Figure 3c). (b, c) Serial transverse sections stained with safranin astra blue (b) and phloroglucin hydrochroric acid (c). (d) A serial transverse section showing autofluorescence.

peak at *m/z* 320.0 were found in the MALDI-TOF CID-FAST spectra of sucrose (Figure 5d). The peaks at *m/z* 185 are likely to have originated from glucose, aldohexopyranose, moiety of coniferin and sucrose, judged by similarity of fragmentation patterns of Figure 5c and d, while the fructose moiety of sucrose would appear at *m/z* 185 as a product ion. The peaks at *m/z* 201 and 202 (coniferin) and *m/z* 203 (sucrose) probably originated from, respectively, coniferyl alcohol moiety (coniferin) and fructose; ketohexofuranose moiety (sucrose). Figure 5e provides the MALDI-TOF CID-FAST spectrum measured from the area showing the abundance of the *m/z* 365 product in a transverse section of differentiating normal wood in *C. obtusa*. The spectrum had two major peaks at *m/z* 185.4 and *m/z* 203.8. Because the area showing precursor ion peak was very limited in the section, it was difficult to sum up enough signals to get minor peaks that are different between coniferin and sucrose. Since sucrose showed a similar precursor ion peak (*m/z* 365 $[M + Na]^+$) and also similar fragmentation pattern except some minor peaks compared with coniferin, it was difficult to distinguish the presence of coniferin and sucrose using MALDI-MSI only.

Osmium tetroxide vapor treatment in MALDI-MSI

A comparison of the chemical structures of coniferin and sucrose reveals that coniferin has a C=C double bond that is lacking in sucrose. Osmium tetroxide is well known to be the most reliable reagent available for the *cis* hydroxylation of alkenes to give the corresponding *cis*-diols (Schröder 1980). Milas et al. (1939) reported the *cis* hydroxylation of cinnamyl alcohol using osmium

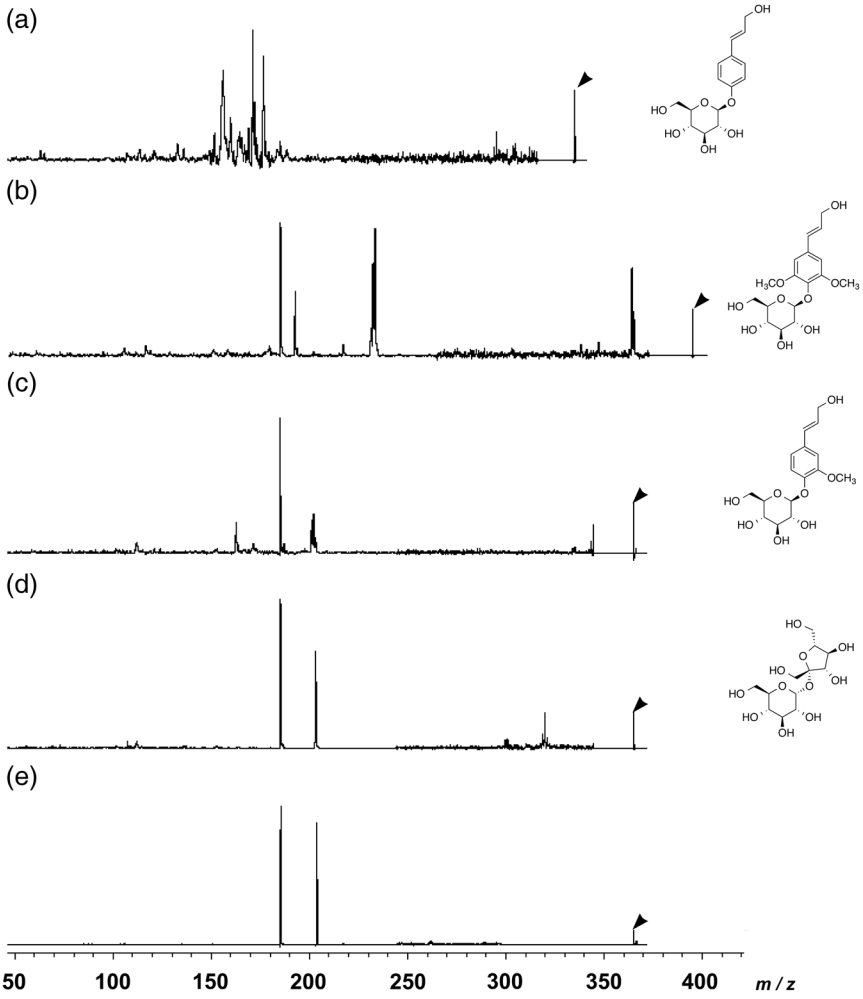

Figure 5. Comparison of MALDI-TOF CID-FAST spectra of the precursor ion at *m/z* 335 from *p*-glucocoumaryl alcohol (a), at *m/z* 395 from syringin (b), at *m/z* 365 from coniferin (c), at m/z 365 from sucrose (d), and at m/z 365 from a transverse section of differentiating xylem in *C. obtusa* normal wood (e). Arrowheads show the peaks of the precursor ions.

tetroxide, which can be used as a vapor. Therefore, in the present study, vapor treatment of osmium tetroxide was applied in MALDI-MSI to distinguish the presence of coniferin and sucrose in differentiating xylem.

Figure 6 shows MALDI-TOF MS spectra of coniferin and sucrose before and after treatment with osmium tetroxide vapor. Coniferin and sucrose showed one distinct peak at *m/z* 365 $[M + Na]^+$ before treatment (Figure 6b and c). After the treatment by osmium tetroxide vapor, the peak shifted to *m/z* 399 (Figure 6d and f), suggesting that two hydroxyl groups were introduced to the Cα–Cβ double bond of coniferin to produce the *threo* form of arylglycerol deriative (Figure 6a). In contrast, no shift was found in sucrose after the treatment with osmium tetroxide vapor (Figure 6e and g). In addition, the peaks of *p*-glucocoumaryl alcohol (*m/z* 335$[M + Na]^+$) and syringin (*m/z* 395 $[M + Na]^+$) also shifted to *m/z* 369 and *m/z* 429, respectively (data not shown).

Images of MALDI-MSI, before and after treatment with osmium tetroxide vapor in differentiating normal woods of *C. obtusa* and *C. japonica*, are shown in Figure 7. Before treatment, an abundance of *m/z* 365 was found in developing xylem during S_2 layer formation (Figure 7a and c), whereas the *m/z* 399 peak was weak, and the *m/z* 399 product was almost absent where *m/z* 365 product was found (Figure 7b and d). After treatment with osmium tetroxide vapor, an abundance of the *m/z* 399 product was found in developing xylem during S_2 layer formation (Figure 7f, h, j and l), suggesting that coniferin should exist there. Even after vapor treatment, an abundance of the *m/z* 365 product was mainly found in developing xylem during S_2 layer formation (Figure 7e, g, i and k), suggesting that sucrose or a small amount of unreacted coniferin may also exist there. For both *C. obtusa* (Figure 8a) and *C. japonica* (Figure 8b), the peaks of *m/z* 365 and *m/z* 399 were distinguishable.

MALDI-MSI of differentiating xylem in compression wood

In compression wood, the peaks of *m/z* 365 and *m/z* 399 (Figure 8c and d) were not so obvious compared with those in normal wood (Figure 8a and b). Figure 9 presents the results of

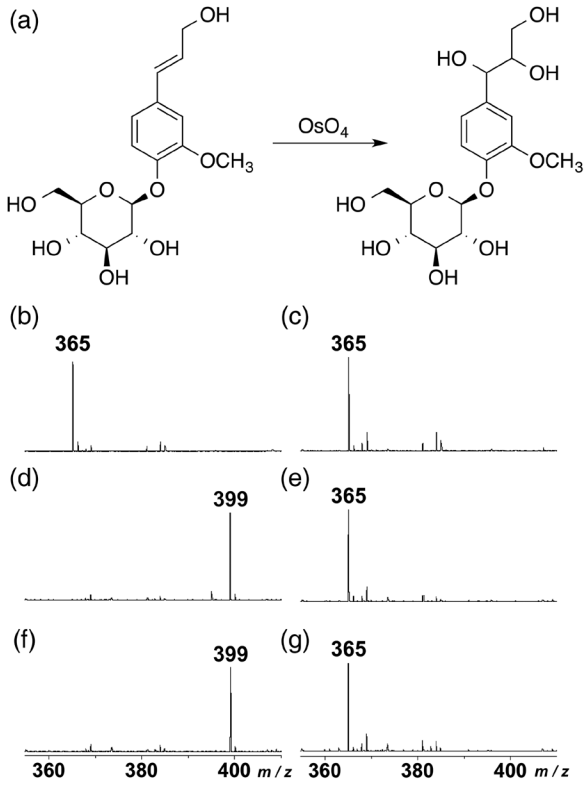

Figure 6. MALDI-TOF MS spectra of coniferin (b, d, f) and sucrose (c, e, g) before and after treatment with osmium tetroxide vapor. (a) A reaction formula during vapor treatment with osmium tetroxide. (b, c) Before treatment, (d, e) after treatment for 24 h at room temperature, and (f, g) after treatment for 48 h at room temperature.

MALDI-MSI analysis of compression wood. After osmium tetroxide vapor treatment, the distribution of the *m/z* 365 and *m/z* 399 products was restricted in the narrow area in an early stage of secondary wall formation (Figure 9a–d). We also obtained an image of the *m/z* 335 (*p*-glucocoumaryl alcohol $[M + Na]^+$), but no obvious distribution in differentiating xylem was found in either *C. obtusa* or *C. japonica* (data not shown).

Discussion

Distribution of coniferin in differentiating normal wood tracheids

Since coniferin and sucrose showed a similar *m/z* peak and their fragmentation patterns were almost similar except for some minor peaks in the CID measurement, it was quite difficult to determine the distribution of coniferin in differentiating xylem using MALDI-MSI only. MALDI-MSI coupled with treatment with osmium tetroxide vapor was very effective in distinguishing coniferin from sucrose in differentiating xylem. Using exactly the same sample *C. obtusa* tree, the results from MALDI-MSI analysis in the present study were similar to the results from Raman microscopy. In both cases, coniferin should exist in normal wood tracheid lumina during S_2 layer formation (Morikawa et al. 2010, Tsuyama et al. 2013). In normal wood of *C. japonica*, MALDI-MSI results coupled with osmium tetroxide vapor treatment were similar to those in normal wood of *C. obtusa*. Overall, the results suggest that coniferin is pooled possibly in vacuoles in differentiating

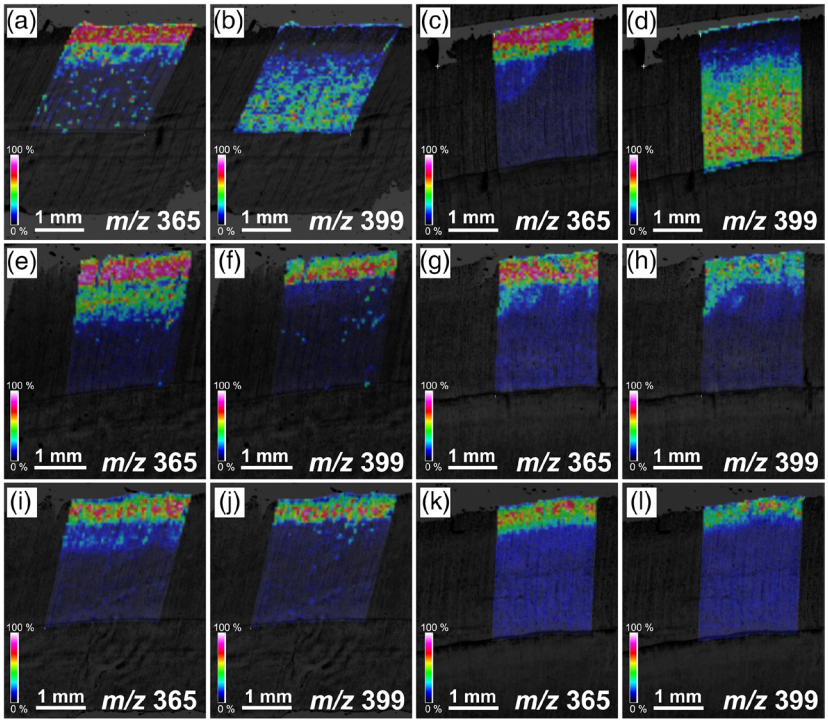

Figure 7. Ion images obtained from MALDI-MSI of transverse sections of differntiating normal woods in *C. obtusa* (a, b, e, f, i, j) and *C. japonica* (c, d, g, h, k, l) before and after the treatment with osmium tetroxide vapor. (a–d) Before treatment, (e–h) after treatment for 24 h at room temperature, and (i–l) after treatment for 48 h at room temperature.

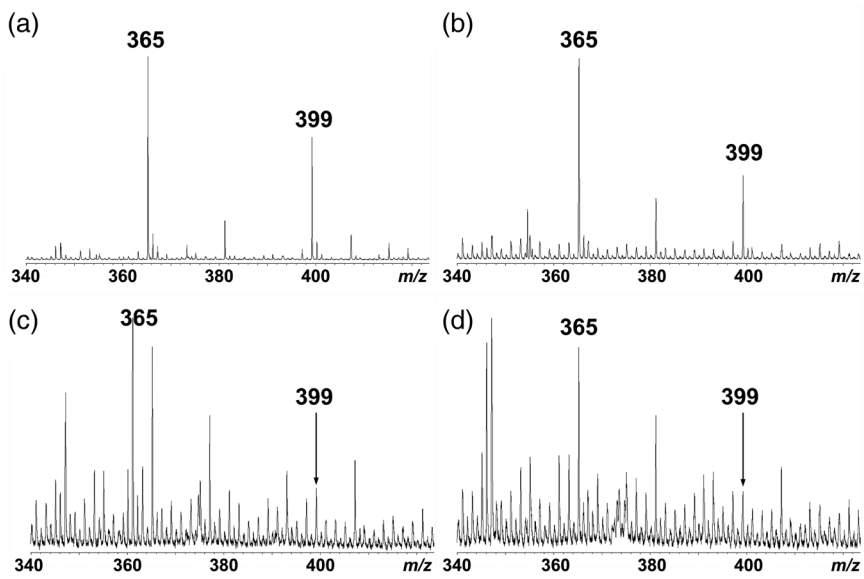

Figure 8. Comparison of MALDI-TOF MS spectra taken from differentiating xylems in normal wood (a) and compression wood (c) in *C. obtusa* and from differentiating xylem in normal wood (b) and compression wood (d) in *C. japonica* after treatment with osmium tetroxide vapor for 24 h at room temperature.

tracheids during S_2 layer formation and then actively transported to the cell wall during or after S_3 layer formation. As existing lignified cell walls showed similar peaks to coniferin in Raman microscopy, the calculation of differential spectrum after normalization is necessary to confirm the existence of coniferin in differentiating xylem, and imaging showing distribution of coniferin was difficult. Although the lateral resolution of images was much lower than from Raman microscopy, the effect of the existing lignified cell wall is negligible under adequate laser power in MALDI-MSI analysis. Therefore, the technique in the present study enabled us to clarify distribution of coniferin in one section from differentiating xylem.

Since it was difficult to prepare 20-μm transverse sections that included phloem, the cambial zone, and differentiating xylem, phloem and the cambial zone were removed before sectioning. The information for secondary phloem, cambial zone and differentiating xylem during primary wall formation was lost in the present study. Work is now in progress to gather information on coniferin distribution in secondary phloem and during the very early stages of lignification.

In transverse sections, ray parenchyma cells were cut longitudinally, and their cell lumina were occasionally opened against the laser in MALDI-MSI. Therefore, distribution of coniferin in ray parenchyma cells remains unclear. Serial tangential sections will be suitable for understanding the distribution of coniferin in ray parenchyma cells.

Distribution of coniferin in differentiating compression wood tracheids

Compression wood is known to have lignin content greater than that in normal wood. A greater amount of monolignol or monolignol glucosides, therefore, must be transported to the lignifying cell walls in compression wood. Our MALDI-MSI analysis coupled with osmium tetroxide vapor treatment showed very restricted distribution of coniferin in differentiating xylem in compression wood, and the corresponding peak after osmium tetroxide vapor treatment was less prominent than in normal wood. Although it is difficult to evaluate the peak height quantitatively in MALDI-TOF MS, our results showed that the distribution of coniferin was less prominent in compression wood than in normal wood. This suggests other mechanisms in which monolignols or monolignol glucosides are not pooled but possibly synthesized and efficiently transported to cell walls just after synthesis.

Although we have tried to detect *p*-glucocoumaryl alcohol, the monolignol glucoside for *p*-hydroxyphenyl lignin, no obvious distribution was shown in compression wood. This also suggests that this glucoside may not be pooled in compression wood unlike coniferin in normal wood.

Conclusion

Matrix-assisted laser desorption/ionization mass spectrometric imaging coupled with osmium tetroxide vapor treatment enabled us to visualize the distribution of coniferin in differentiating normal and compression woods of *C. obtusa* and *C. japonica*. Coniferin was distributed in developing tracheids during S_2 layer formation in normal wood. In compression wood, the distribution of coniferin was less prominent than the distribution in normal wood. The technique used in the present study will be effective for visualizing distribution of monolignol glucosides in differentiating xylem of various tree species.

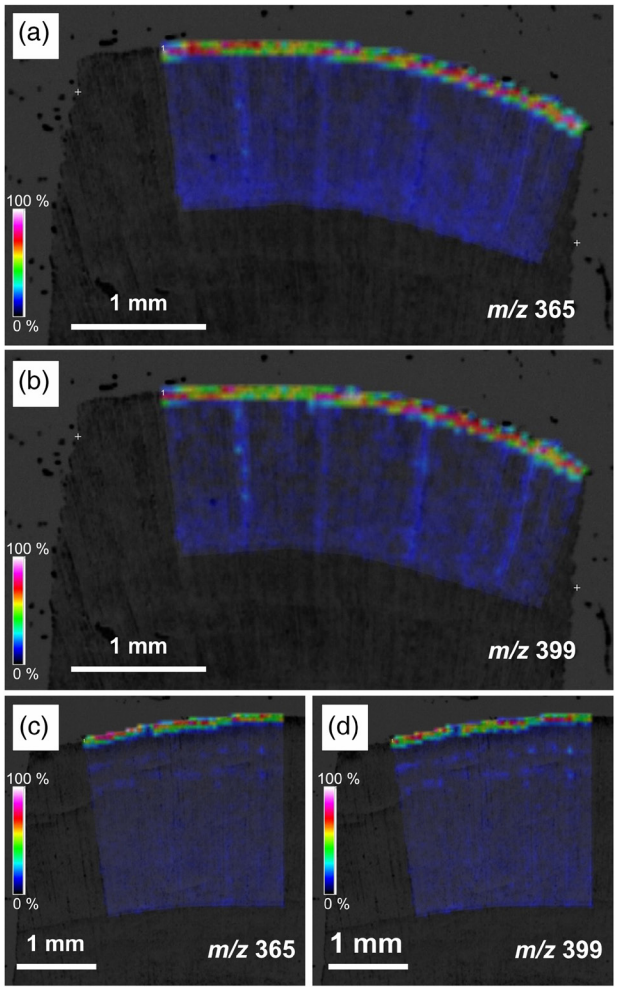

Figure 9. Ion images obtained from MALDI-MSI of transverse sections of differntiating compression woods in *C. obtusa* (a, b) and *C. japonica* (c, d) after treatment with osmium tetroxide vapor for 24 h at room temperature.

Acknowledgments

The authors are indebted to Professor Emeritus Noritsugu Terashima, Nagoya University, Japan, for kindly donating *p*-glucocoumaryl alcohol, coniferin and syringin.

Conflict of interest

None declared.

Funding

This work was supported by KAKENHI, a Grant in Aid for Scientific Research (C) (No. 22580183) from the Japan Society for the Promotion of Science (JSPS).

References

Araújo P, Ferreira MS, de Oliveira DN, Pereira L, Sawaya ACHF, Catharino RR, Mazzafera P (2014) Mass spectrometry imaging: an expeditious and powerful technique for fast *in situ* lignin assessment in *Eucalyptus*. Anal Chem 86:3415–3419.

Chapelle A, Morreel K, Vanholme R, Le-Bris P, Morin H, Lapierre C, Boerjan W, Jouanin L, Demont-Caulet N (2012) Impact of the absence of stem-specific β-glucosidases on lignin and monolignols. Plant Physiol 160:1204–1217.

Dharmawardhana DP, Ellis BE, Carlson JE (1995) A beta-glucosidase from lodgepole pine xylem specific for the lignin precursor coniferin. Plant Physiol 107:331–339.

Freudenberg K, Harkin JM (1963) The glucosides of cambial sap of spruce. Phytochemistry 2:189–193.

Freudenberg K, Torres-Serres J (1967) Conversion of phenylalanine into lignin-forming glucosides. Justus Liebigs Ann Chem 703:225–230.

Fukushima K, Terashima N (1991) Heterogeneity in formation of lignin. Part XV: formation and structure of lignin in compression wood of *Pinus thunbergii* studied by microautoradiography. Wood Sci Technol 25:371–381.

Fukushima K, Taguchi S, Matsui N, Yasuda S (1997) Distribution and seasonal changes of monolignol glucosides in *Pinus thunbergii*. Mokuzai Gakkaishi 43:254–259.

Hösel W, Todenhagen R (1980) Characterization of a β-glucosidase from *Glycine max* which hydrolyses coniferin and syringin. Phytochemistry 19:1349–1353.

Imagawa H, Fukazawa K, Ishida S (1976) Study on the lignification in tracheids of Japanese larch, *Larix leptolepis* GORD. Res Bull Coll Exp For Hokkaido Univ 33:127–138 (in Japanese).

Jung S, Foston M, Kalluri UC, Tuskan GA, Ragauskas AJ (2012) 3D chemical image using TOF-SIMS revealing the biopolymer component spatial and lateral distributions in biomass. Angew Chem Int Ed 51:12005–12008.

Kaspar S, Peukert M, Svatos A, Matros A, Mock H-P (2011) MALDI-imaging mass spectrometry—an emerging technique in plant biology. Proteomics 11:1840–1850.

Kutscha NP, Schwarzmann JM (1975) The lignification sequence in normal wood of balsam fir (*Abies balsamea*). Holzforschung 29:79–84.

Li Z, Bohn PW, Sweedler JV (2010) Comparison of sample pre-treatments for laser desorption ionization and secondary ion mass spectrometry imaging of *Miscanthus* × *giganteus*. Bioresour Technol 101:5578–5585.

Liu C-J (2012) Deciphering the enigma of lignification: precursor transport, oxidation, and the topochemistry of lignin assembly. Mol Plant 5:304–317.

Lunsford KA, Peter GF, Yost RA (2011) Direct matrix-assisted laser desorption/ionization mass spectrometric imaging of cellulose and hemicellulose in populus tissue. Anal Chem 83:6722–6730.

Marcinowski S, Falk H, Hammer DK, Hoyer B, Grisebach H (1979) Appearence and localization of a β-glucosidase hydrolyzing coniferin in spruce (*Picea abies*) seedlings. Planta 144:161–165.

Marjamaa K, Lehtonen M, Lundell T, Toikka M, Saranpää P, Fagerstedt KV (2003) Developmental lignification and seasonal variation in β-glucosidase and peroxidase activities in xylem of Scots pine, Norway spruce and silver birch. Tree Physiol 23:977–986.

Milas NA, Sussman S, Mason HS (1939) The hydroxylation of unsaturated substances. V. The catalytic hydroxylation of certain unsaturated substances with functional groups. J Am Chem Soc 61:1844–1847.

Morikawa Y, Yoshinaga A, Kamitakahara H, Wada M, Takabe K (2010) Cellular distribution of coniferin in differentiating xylem of *Chamaecyparis obtusa* as revealed by Raman microscopy. Holzforschung 64:61–67.

Peukert M, Matros A, Lattanzio G, Kaspar S, Abadía J, Mock H-P (2012) Spatially resolved analysis of small molecules by matrix-assisted laser desorption/ionization mass spectrometric imaging (MALDI-MSI). New Phytol 193:806–815.

Samuels A, Rensing K, Douglas C, Mansfield S, Dharmawardhana D, Ellis B (2002) Cellular machinery of wood production: differentiation of secondary xylem in *Pinus contorta* var. *latifolia*. Planta 216:72–82.

Savidge RA, Forster H (1998) Seasonal activity of uridine 5′-diphosphoglucose: coniferyl alcohol glucosyltransferase in relation to cambial growth and dormancy in conifers. Can J Bot 76:486–493.

Schmid G, Hammer DK, Ritterbusch A, Grisebach H (1982) Appearance and immunohistochemical localization of UDP-glucose: coniferyl alcohol glucosyltransferase in spruce (*Picea abies* (L.) Karst.) seedlings. Planta 156:207–212.

Schröder M (1980) Osmium tetraoxide cis hydroxylation of unsaturated substrates. Chem Rev 80:187–213.

Steeves V, Förster H, Pommer U, Savidge R (2001) Coniferyl alcohol metabolism in conifers—I. Glucosidic turnover of cinnamyl aldehydes by UDPG: coniferyl alcohol glucosyltransferase from pine cambium. Phytochemistry 57:1085–1093.

Takabe K, Fujita M, Harada H, Saiki H (1981*a*) The deposition of cell wall components in differentiating tracheids of Sugi. Mokuzai Gakkaishi 27:249–255 (in Japanese).

Takabe K, Fujita M, Harada H, Saiki H (1981*b*) Lignification process of Japanese black pine (*Pinus thunbergii* Parl.) tracheids. Mokuzai Gakkaishi 27:813–820 (in Japanese).

Takabe K, Fujita M, Harada H, Saiki H (1985) Autoradiographic investigation of lignification in the cell walls of Cryptomeria (*Cryptomeria japonica* D. Don). Mokuzai Gakkaishi 31:613–619.

Takabe K, Fujita M, Harada H, Saiki H (1986) Lignification process in Cryptomeria (*Cryptomeria japonica* D. Don) tracheid: electron microscopic observation of lignin skeleton of differentiating xylem. Res Bull Coll Exp For Hokkaido Univ 43:783–788.

Terashima N, Fukushima K (1988) Heterogeneity in formation of lignin—XI: an autoradiographic study of the heterogeneous formation and structure of pine lignin. Wood Sci Technol 22:259–270.

Terazawa M, Okuyama H, Miyake M (1984) Phenolic compounds in living tissues of woods I. Phenolic beta-glucosides of 4-hydroxycinnamyl alcohol derivatives in the cambial sap of woods. Mokuzai Gakkaishi 30:322–328.

Tsuyama T, Kawai R, Shitan N, Matoh T, Sugiyama J, Yoshinaga A, Takabe K, Fujita M, Yazaki K (2013) Proton-dependent coniferin transport, a common major transport event in differentiating xylem tissue of woody plants. Plant Physiol 162:918–926.

Wardrop AB (1957) The phase of lignification in the differentiation of wood fibers. Tappi 40:225–243.

Ye H, Germperline E, Venkateshwaran M, Chen R, Delaux P-M, Howes-Podoll M, Ané J-M, Li L (2013) MALDI mass spectrometry-assisted molecular imaging of metabolites during nitrogen fixation in the *Medicago truncatula—Sinorhizobium meliloti* symbiosis. Plant J 75:130–145.